



# An in-depth analysis of the silicon solar cell key parameters' optimal magnitudes using PC1D simulations



Xiyang Cai, Xinjie Zhou, Ziyi Liu, Fengjing Jiang, Qingchun Yu\*

School of Mechanical Engineering, Shanghai Jiao Tong University, Shanghai 200240, PR China

## ARTICLE INFO

### Article history:

Received 26 January 2018

Accepted 27 February 2018

### Keywords:

Silicon solar cell

PC1D

Thickness

Dopant density

Carrier transmission

## ABSTRACT

In this study, the optimal magnitudes of silicon solar cell key parameters were calculated and verified using the PC1D simulation program. By varying the parameters such as emitter thickness, base thickness, emitter dopant density and base dopant density, the corresponding I–V curves were generated. According to open circuit voltage ( $V_{oc}$ ) and short circuit current ( $I_{sc}$ ) in I–V curves, the optimum magnitudes of these parameters were determined. The results were validated by investigating the factors related to the carrier transmission mechanism including diffusion length, minority carrier lifetime, photogeneration and conductivity in a cell. Hence, the paper demonstrates the best magnitudes for emitter thickness, base thickness, emitter dopant density and base dopant density are 0.1  $\mu\text{m}$ , 100  $\mu\text{m}$ ,  $10^{20} \text{ cm}^{-3}$  and  $5 \times 10^{16} \text{ cm}^{-3}$  respectively. Furthermore, the optimized parameters obtained from simulations show good agreement with corresponding values of one commercial crystalline solar cell. The study proves that PC1D can provide reliable reference values for solar cell design process.

© 2018 Elsevier GmbH. All rights reserved.

## 1. Introduction

Since the 21st century, humankind is facing increasingly complex environmental issues and serious energy crisis. In world's energy market, solar cell is playing an essential role due to its sustainable and clean character. Silicon solar cell, by virtue of its high efficiency and economy, dominates the solar cell market. The performance improvement of silicon solar cells, as its high value to energy saving and environmental protection, is a permanent goal the photovoltaic researchers pursue across the globe.

The science community and industry circles have made great progress in the research of silicon solar cell in recent years. Descoedres et al. compared the performances of n-type and p-type Wafers silicon heterojunction cells by experiments and pointed out that p-type wafers perform worse than n-type in the low-carrier-injection range [1]. Richter et al. discovered the Limiting Efficiency of the crystalline silicon solar cells and inferred the figure of maximum theoretical efficiency for a 110  $\mu\text{m}$  thick silicon solar cell [2]. Masuko et al. developed a crystalline silicon heterojunction solar cell with more than 25% conversion efficiency [3]. Battaglia et al. summarized that passivating contacts and dopant-free electron and hole contacts are two major emerging concepts and technologies for further development [4]. The large gap between realistic cell and theoretical cell, various essential concepts, and numerous emerging technologies indicate the research of silicon solar cells is still necessary.

\* Corresponding author.

E-mail address: [qcyu@sjtu.edu.cn](mailto:qcyu@sjtu.edu.cn) (Q. Yu).

As an important complement to experiment, numerical simulation, represented by PC1D, provides schemes and corresponding estimated results for the experiment [5–9]. PC1D was verified to be reliable and effective in the research of solar cell in previous literatures. Sato et al. performed the degradation modeling of a three-junction solar cells subjected to proton irradiation with the use of PC1D and the values of  $I_{sc}$  and  $V_{oc}$  obtained from the calculations showed good agreement with experimental values at an accuracy of 5% [10]. A series of numerical modeling of crystalline silicon solar cells was reviewed by Altermatt and indicated the strong influence of PC1D to PV community [11]. Sepeai et al. applied the PC1D to determine the orders of magnitude of various parameters including emitter doping, bulk doping, BSF doping, minority carrier lifetime, wafer thickness, front and rear surface recombination to obtain the optimum efficiency of the bifacial solar cell [12]. Belarbi et al. made several simulations with PC1D to see the influence of various parameters including surface, thickness and doping on the efficiency of solar cells [13]. Nawale et al. deeply investigated the thickness factor with PC1D and revealed that the p-type thickness,  $I_{sc}$  and  $V_{oc}$  are the best parameters to model the silicon solar cell through statistical analysis [14]. Panek used PC1D to analyze the influence of a p-type Si with different resistivity, charge carrier lifetime on external quantum efficiency for Si based solar cell [15]. The simulation method with PC1D has been widely used in the research field of solar cells.

The application of computer programs to model the solar cell can improve the experimental reliability as well as save time and costs. This study first applied the PC1Dmod Ver.6.2 to plot a set of I–V curves by varying the parameters including emitter thickness, base thickness, emitter dopant density and base dopant density. According to open circuit voltage ( $V_{oc}$ ) and short circuit current ( $I_{sc}$ ) in I–V curves, the optimum magnitudes of these parameters were determined. As an indispensable verification of the results above, intensive analysis of the carrier transmission mechanisms, which control the performance of silicon solar cells, was further investigated. Finally, the simulation results were compared with a commercial photovoltaic product. These three parts construct systematic analysis on the photovoltaic cell's design parameters.

## 2. Introduction to PC1D and solution equations

In this section, the principles of PC1D are introduced, which are the basis for simulation calculation.

Among the various simulation programs, PC1D is the most widely used in photovoltaic research, teaching and engineering. PC1D, short for Personal Computer One Dimension, is a finite-element program for modeling semiconductor devices. The first version of PC1D was released in 1985, followed by multiple versions with more powerful functionalities in the next 30 years. The study was accomplished by PC1Dmod Ver.6.2. Issued in December 2016, PC1Dmod Ver.6.2 is the latest version so far. A team led by Halvard Haug from Institute for Energy Technology (Norway) is continuing to release the unofficial, modified version of PC1D [16].

PC1D is fundamentally an equation solver. By solving five basic equations, it obtains parameters that describe the crystalline Si solar cell.

$$J_n = \mu_n \cdot n \cdot \nabla E_{Fn} \quad (1)$$

$$J_p = \mu_p \cdot p \cdot \nabla E_{Fp} \quad (2)$$

$$\frac{\partial n}{\partial t} = \frac{\nabla \cdot J_n}{q} + G_L - U_n \quad (3)$$

$$\frac{\partial p}{\partial t} = \frac{\nabla \cdot J_p}{q} + G_L - U_p \quad (4)$$

$$\Delta^2 \phi = \frac{q}{\varepsilon} (n - p + N_{acc}^- - N_{don}^+) \quad (5)$$

Eqs. (1) and (2) are transport equations, characterizing electron and hole current density. The electron and hole current density ( $J_n, J_p$ ) are impacted by variables including the electron/hole density ( $n, p$ ), the electron/hole mobility ( $\mu_n, \mu_p$ ), and the electron/hole quasi-Fermi energies ( $E_{Fn}, E_{Fp}$ ). Eqs. (3) and (4) are continuity equations, describing the derivative of  $n, p$  versus time ( $t$ ).  $G_L$  denotes the volume generation rate, representing the absorption of light. Recombination of electrons and holes ( $U_n, U_p$ ) are always the same in two-carrier model because the electrons and holes are created and annihilated in pairs. Eq. (5) is Poisson's equation.  $\psi, \varepsilon$  and  $\rho$  stand for electrostatic potential, permittivity and volume charge density. Four types of charge concentration contribute to volume charge density, i.e., electron density, hole density, the concentration of ionized donor impurity and concentration of ionized acceptor impurity. In addition, charge carrier statistics are necessary. They are provided by Eqs. (6) and (7).

$$n = N_C F_{1/2} \left( \frac{q\psi + V_n - q\phi_{n,i} + \ln(n_i, q/N_C)}{k_B T} \right) \quad (6)$$

$$p = N_V F_{1/2} \left( \frac{-q\psi + V_p + q\phi_{p,i} + \ln(p_i, q/N_V)}{k_B T} \right) \quad (7)$$

**Table 1**  
Origin case parameters for the simulation.

Parameters	Values
Emitter thickness	0.10 $\mu\text{m}$
Base thickness	100 $\mu\text{m}$
Emitter dopant density	$10^{19} \text{cm}^{-3}$
Base dopant density	$5 \times 10^{15} \text{cm}^{-3}$
Temperature	25°
Device area	250 $\text{cm}^2$
Band gap	1.124 eV
Intrinsic carrier density	$9.56 \times 10^9 \text{cm}^{-3}$ [17]
Exterior front reflectance	5%
Bulk recombination	$\tau_n = \tau_p = 250 \mu\text{s}$
Front-surface recombination	100,000 $\text{cm s}^{-1}$
Rear-surface recombination	100 $\text{cm s}^{-1}$
Front surface texture angle	45°
Front surface texture depth	2.5 $\mu\text{m}$
Constant intensity	0.1 $\text{W cm}^{-2}$
Spectrum	AM 1.5G

Apart from thickness and dopant density, variables are consistent with that of the commercial solar cell, which is a precondition for comparison between simulation results and the commercial solar cell.

$N_C$ ,  $N_V$  are the effective density of states in the conduction and valence bands.  $F_{1/2}$  represents the complete Fermi integral of order 1/2.  $(V_n, V_p)$ ,  $(\phi_{n,i}, \phi_{p,i})$ ,  $n_{i,0}$ ,  $k_B$  and  $T$  are the band-edge potentials, quasi-Fermi potentials, intrinsic carrier density, Boltzmann constant and temperature. Based on Eqs. (6) and (7), the problem is simplified to the solution of five unknowns including two current densities ( $J_n, J_p$ ), two quasi-Fermi potentials ( $E_{Fn}, E_{Fp}$ ) and electrostatic potential ( $\psi$ ). It is sufficient to solve the five initial equations with appropriate boundary conditions for the simulations of crystalline Si solar cells.

### 3. Simulations and results

In Si solar cell fabricating process, emitter (n-type) thickness, base (p-type) thickness, emitter (n-type) dopant density and base (p-type) dopant density are the most important parameters. Identifying the magnitudes of these parameters is a prerequisite for a prominent cell. However, these four parameters usually differ by 2–4 orders of magnitude. Hence, doing experiments can be a very costly method in the process to find out parameter's best magnitude. In comparison, simulation by PC1D is a cheap and efficient method. In the following part, we use PC1D to determine parameters' optimal magnitude of the solar cell and develop a deeper understanding of how these factors affect solar cell's performance.

The settings and parameters of the "origin case" are shown in Table 1. All cases were generated based on "origin case" by changing only one parameter.

#### 3.1. Determination of the optimum emitter thickness magnitude

In a typical solar cell, emitter thickness only accounts for 0.6%–10% of total thickness [14]. To probe its influence on cell's performance, we varied the emitter thickness from 0.01  $\mu\text{m}$  to 10  $\mu\text{m}$  while the other parameters were kept unchanged.

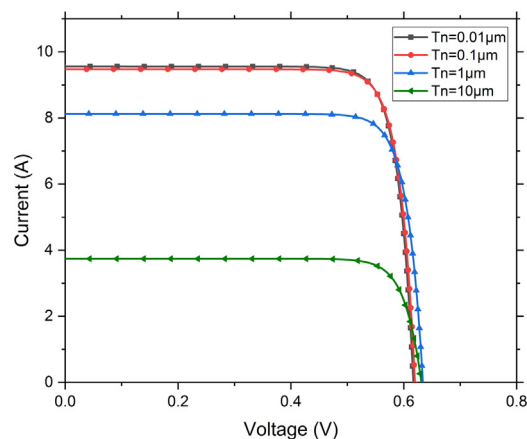


**Fig. 1.** Influence of variation in the emitter thickness on I–V characteristic.

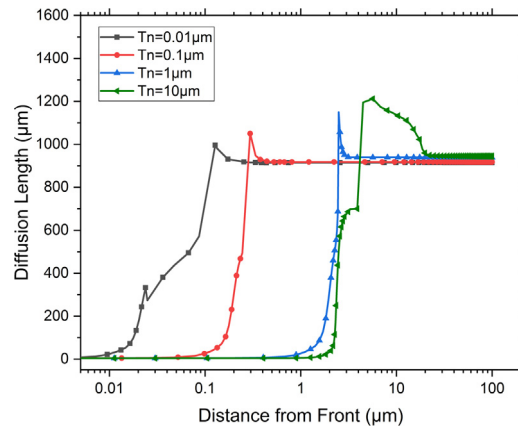


Fig. 2. Influence of variation in the emitter thickness on diffusion length.

Four different I–V curves are shown in Fig. 1. The result reveals an inverse relationship between emitter thickness and short circuit current ( $I_{sc}$ ). It can be also observed that  $I_{sc}$  increases dramatically as emitter thickness ( $T_n$ ) decreases from 10  $\mu\text{m}$  to 0.1  $\mu\text{m}$ . By contrast, there is just a slight improvement in  $I_{sc}$  when emitter thickness is reduced from 0.1  $\mu\text{m}$  to 0.01  $\mu\text{m}$ .

Usually, the emitter region is much more heavily doped than base region by 2–3 orders of magnitude, leading to high recombination in the emitter. High recombination means short diffusion length. Diffusion length, which is an important parameter for performance of solar cells, is defined as the average distance that carriers can travel from generation point before they recombine [18]. Fig. 2 illustrates minority carriers' diffusion length across the whole cell. Diffusion length in emitter region is about 4  $\mu\text{m}$ , much shorter than base region's. The decrease of diffusion length in emitter region is attributed to the high dopant densities of the emitter. On the other hand, collection probability (probability that a light-generated carrier is collected by p–n junction) is a function of diffusion length and device dimension [19]. If emitter thickness is more than a diffusion length away from the junction, the collection probability is quite low. If emitter thickness is one or more orders lower than diffusion length, the collection probability substantially increase. Higher collection probability means more light-generated carriers are collected by p–n junction and are conducted out the cell. Hence,  $I_{sc}$  increases with the decrease of emitter thickness.

Therefore, emitter thickness magnitude should be maintained at about 0.1  $\mu\text{m}$ . Higher orders of emitter thickness magnitude results in loss of  $I_{sc}$  by increasing recombination and lower orders of emitter thickness magnitude may slightly increase cell's performance but does harm to cell's life span and durability.

### 3.2. Determination of the optimum base thickness magnitude

In parallel to the study based on the effect of variation of emitter thickness above, three cases with different thicknesses of the base ( $T_p$ ) were simulated with PC1D, and the results were arranged to plot Figs. 3 and 4.

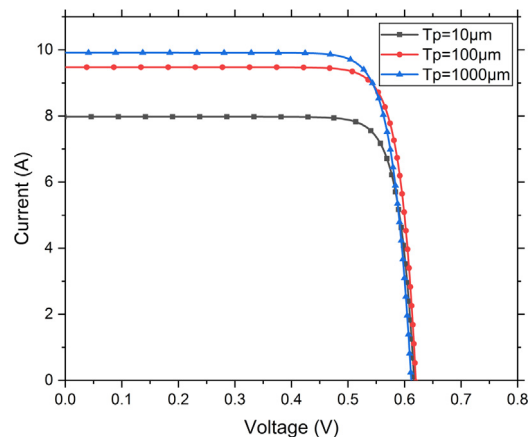


Fig. 3. Influence of variation in the base thickness on I–V characteristic.

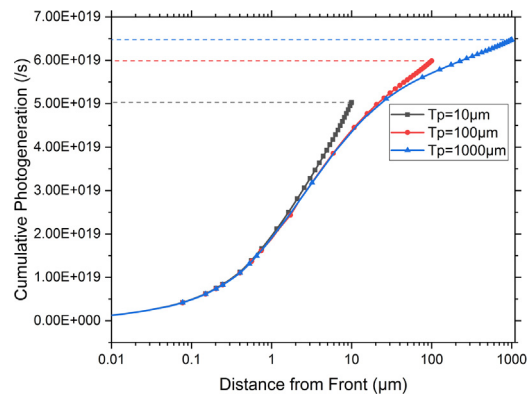


Fig. 4. Influence of variation in the base thickness on photogeneration.

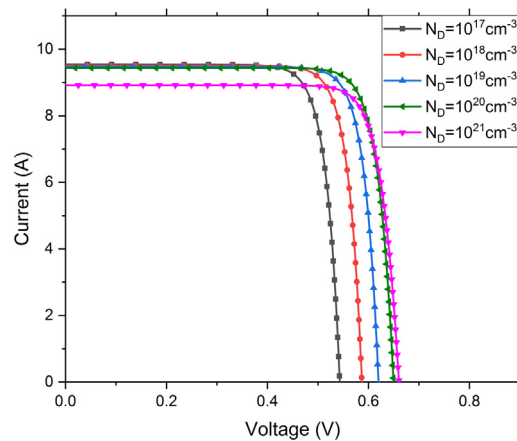


Fig. 5. Influence of variation in the emitter dopant densities on I–V characteristic.

Fig. 3 suggests that short circuit current increases with the growth of base thickness. With base thickness increasing, more photons are absorbed by cell (instead of penetrating cell), exciting more electrons into the conduction band resulting in higher  $I_{sc}$ . Fig. 4 shows the relationship between cumulative photogeneration and base thickness. In Fig. 4, cumulative photogeneration is minimum at a base thickness of 10  $\mu\text{m}$ . Then, it grows slowly with increase of base thickness and reaches its top at the thickest point.

In short, in order to gain enough photons to excite electron-hole pairs, a certain base thickness is required. However, high resistance and high cost emerge in a thicker cell. So, base thickness magnitude should be kept at about 100  $\mu\text{m}$ .

### 3.3. Determination of the optimum emitter doping magnitude

Even though there have been many kinds of different solar cells, doping is always the core procedure in production. Regarded as the main reason to trigger Auger and Shockley-Read-Hall recombination, doping introduces crystal defects into the cell. But doping is also an indispensable means to create depletion region and increase the conductivity of semiconductor which are essential to a high-efficiency solar cell.

To find out how emitter dopant density affects cell's performance, on the base of origin case, five cases with different concentrations of donor atoms were designed. From Fig. 5, it is observed that highest  $V_{oc}$  is obtained at the emitter dopant density of  $10^{21} \text{ cm}^{-3}$  and decreases as emitter dopant density ( $N_D$ ) decrease from  $10^{21} \text{ cm}^{-3}$  to  $10^{17} \text{ cm}^{-3}$ . For simulation reported here,  $I_{sc}$  is almost unchanged from dopant density of  $10^{17} \text{ cm}^{-3}$  to  $10^{20} \text{ cm}^{-3}$  but decreases to a minimum value at the concentration of  $10^{21} \text{ cm}^{-3}$ .

In Fig. 6, the diffusion length of emitter region at concentrations of  $10^{17} \text{ cm}^{-3}$ ,  $10^{18} \text{ cm}^{-3}$ ,  $10^{19} \text{ cm}^{-3}$ ,  $10^{20} \text{ cm}^{-3}$  and  $10^{21} \text{ cm}^{-3}$  are about 180  $\mu\text{m}$ , 40  $\mu\text{m}$ , 4  $\mu\text{m}$ , 0.4  $\mu\text{m}$  and 0.03  $\mu\text{m}$  respectively. Minority carrier lifetime, defined as the average time for recombination to occur after electron-hole generation, is roughly proportional to diffusion length [20]. It is observed that minority carrier lifetime of emitter region at concentrations of  $10^{17} \text{ cm}^{-3}$ ,  $10^{18} \text{ cm}^{-3}$ ,  $10^{19} \text{ cm}^{-3}$ ,  $10^{20} \text{ cm}^{-3}$  and  $10^{21} \text{ cm}^{-3}$  are about 40  $\mu\text{s}$ , 3  $\mu\text{s}$ , 0.04  $\mu\text{s}$ ,  $4 \times 10^{-4} \mu\text{s}$  and  $4 \times 10^{-6} \mu\text{s}$  respectively. At heavily doped emitter, the diffusion length and minority carrier lifetime are lower by 4 orders of magnitude. At lower diffusion length, a large part of electrons are combined with holes before they reach p-n junction. These electrons should have been directed to the external circuit

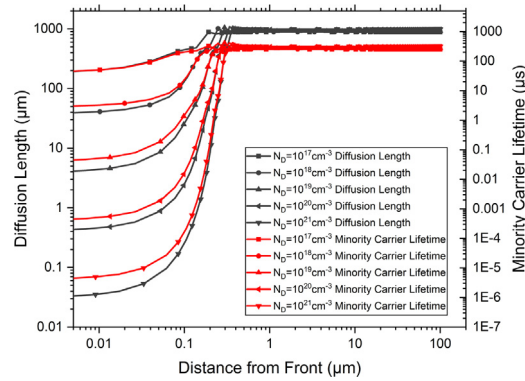


Fig. 6. Influence of variation in the emitter dopant densities on diffusion length and minority carrier lifetime.

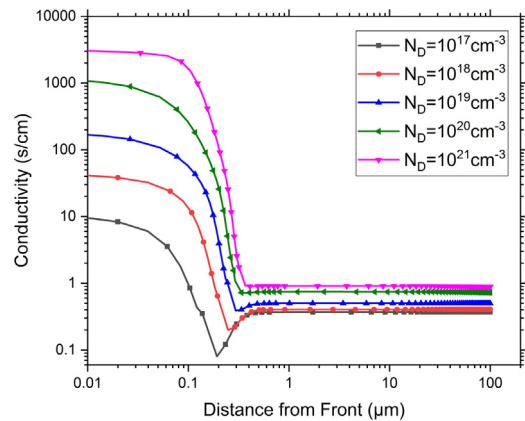


Fig. 7. Influence of variation in the emitter dopant densities on conductivity.

instead of being depleted within the cell. Overall this part demonstrates that decrease of  $I_{sc}$  is due to recombination caused by the heavily doped emitter.

It is also necessary to note that in p-type base region, lines of diffusion length/minority carrier lifetime almost coincide. This is because dopant density is uniform in p-type region among all cells. But in n-type region, the lines separate when dopant densities differentiate.

As shown in Fig. 5,  $V_{oc}$  increase is with the growth of dopant density from  $10^{17}\text{ cm}^{-3}$  to  $10^{21}\text{ cm}^{-3}$ . Fig. 7 illustrates dopant density's impact on conductivity which is the main reason for variation of  $V_{oc}$ . Reduction of emitter dopant density leads to lower conductivity in n-type region, and when conductivity drops, internal series resistance increases. According to Ohm's law, the internal voltage drop of cell increases with the increase of internal series resistance at the same current, directly leading to loss of  $V_{oc}$ . It is important to point out that since high doping narrows the bandgap, increasing doping to increase  $V_{oc}$  becomes counter-productive after a certain limit is reached [12].

As a conclusion, for emitter doping, diffusion length and conductivity should be both taken into account and the optimal magnitude is about  $10^{20}\text{ cm}^{-3}$ .

### 3.4. Determination of the optimum base doping magnitude

The mechanism of base dopant density on the cell is similar to that of emitter doping. Five I–V curves with different base dopant densities are displayed in Fig. 8. As shown in Fig. 8, I–V characterization gradually improves and reaches its best at base dopant density ( $N_A$ ) of  $5 \times 10^{16}\text{ cm}^{-3}$  and then deteriorates at a concentration of  $5 \times 10^{17}\text{ cm}^{-3}$ .

Fig. 9 exemplifies the diffusion length and minority carrier lifetime as base dopant density varies from  $5 \times 10^{13}\text{ cm}^{-3}$  to  $5 \times 10^{17}\text{ cm}^{-3}$ . Unlike Fig. 6, as base dopant density varies from  $5 \times 10^{13}\text{ cm}^{-3}$  to  $5 \times 10^{17}\text{ cm}^{-3}$ , the value of diffusion length and minority carrier lifetime change just within two orders of magnitude. Furthermore, there is little change in diffusion length and minority carrier lifetime of the base region from dopant density of  $5 \times 10^{13}\text{ cm}^{-3}$  to  $5 \times 10^{16}\text{ cm}^{-3}$ . That accounts for the similarity among I–V curves at this range. However, diffusion length and minority carrier lifetime of base region drop significantly and meet their minimum values at a dopant concentration of  $5 \times 10^{17}\text{ cm}^{-3}$ , leading to deterioration of I–V curve.

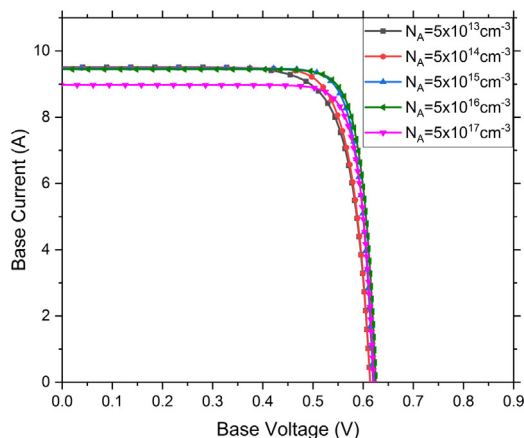


Fig. 8. Influence of variation in the base dopant densities on I–V characteristic.

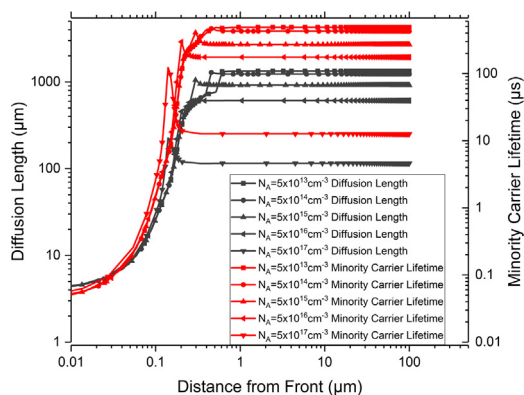


Fig. 9. Influence of variation in the base dopant densities on diffusion length and minority carrier lifetime.

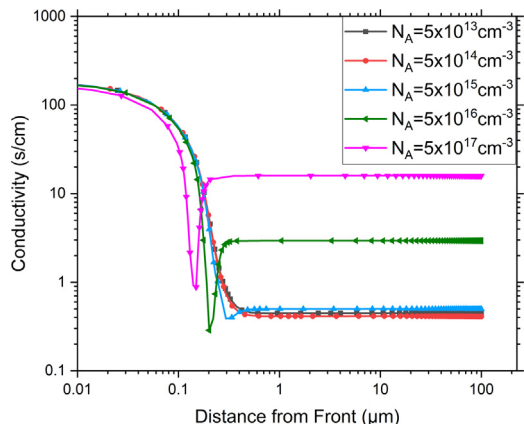


Fig. 10. Influence of variation in the base dopant densities on conductivity.

It is important to point out that lines of diffusion length/minority carrier lifetime coincide in n-type emitter region but stagger in p-type base region. Figs. 6 and 9 suggest that diffusion length and minority carrier lifetime are all negatively associated with doping.

Fig. 10 shows the conductivity of solar cell when base dopant density changes from  $5 \times 10^{13} \text{ cm}^{-3}$  to  $5 \times 10^{17} \text{ cm}^{-3}$ . Base dopant density's influence on conductivity is limited at  $5 \times 10^{13}$ – $5 \times 10^{15} \text{ cm}^{-3}$ . So, in the same analogy, I–V curves are similar at this range.

Therefore, base dopant densities should be lower than  $5 \times 10^{17} \text{ cm}^{-3}$  because of recombination and in order to gain higher conductivity, dopant densities are supposed to be in a higher range. So,  $5 \times 10^{16} \text{ cm}^{-3}$  is a suitable magnitude.

**Table 2**  
Parameters of the “optimal simulated case” and the commercial solar cell.

parameter	“optimal simulated case”	commercial solar cell	comparison
Emitter thickness	0.1 $\mu\text{m}$	0.25–0.45 $\mu\text{m}$	On the same order of magnitude
Base thickness	100 $\mu\text{m}$	190 $\mu\text{m}$	
Emitter doping	$10^{20} \text{ cm}^{-3}$	$1.96\text{--}5.23 \times 10^{19} \text{ cm}^{-3}$	The numerical difference is less than 5%
Base doping	$5 \times 10^{16} \text{ cm}^{-3}$	$1.51 \times 10^{16} \text{ cm}^{-3}$	
FF	84.06%	80.16%–80.55%	
$I_{sc}$	9.41	8.954–9.101 A	
$V_{oc}$	0.6661	0.6342–0.6374 V	

**Table 3**  
Key parameters’ magnitude and constrain factors.

parameter	Optimal Magnitude	Excessive magnitude	Inadequate magnitude
Emitter thickness	0.1 $\mu\text{m}$	High recombination	Low durability
Base thickness	100 $\mu\text{m}$	High cost	Low generation rate
Emitter doping	$10^{20} \text{ cm}^{-3}$	High recombination	High resistance
Base doping	$5 \times 10^{16} \text{ cm}^{-3}$	High recombination	High resistance

#### 4. Contrast and verify

In order to prove the reliability of the calculations, the parameters of a commercial crystalline solar cell, provided by the company SUMEC Group Corporation, are compared with simulation results. As shown in Table 2, the key parameters of the “optimal simulated case” are all on the same order of magnitude with the corresponding parameters of the commercial solar cell. It strongly supports that PC1D is competent to provide reliable reference values for solar cell fabricating process at a lower cost of money and time. Furthermore, FF,  $I_{sc}$  and  $V_{oc}$  of the simulation and the actuality are similar in the same illumination condition. The numerical difference of cell’s performance between the “optimal simulated case” and the commercial solar cell is less than 5%. It validates that results of the simulation are credible.

Another virtue of PC1D is that it exhibits the mechanism of process parameters’ effects on the performance of solar cell. It helps to develop a deeper understanding of cell operating principle. As shown in the Table 3, every process parameter has its own optimal magnitude. But the optimal values of different parameters can differ by 3–4 orders of magnitude. In fact the determination of solar cell’s parameters is the process of balancing the impact of various factors. Recombination, durability, cost and photogeneration are all related to emitter or base thickness. High emitter thickness causes high recombination. Low emitter thickness decreases recombination but may damage the durability. High base thickness helps to make the best of photons but increases the production costs. Low base thickness saves the costs at the expense of low generation rate. So the optimal magnitude of thickness is the one which can balance the effect of all related factors. Similarly, recombination and conductivity are both positively related to dopant density. High conductivity makes contributions to cell’s performance while high recombination deteriorates cell’s performance. Hence, the optimal magnitude of dopant density is the best point in balancing the effect of conductivity and recombination. The results are denoted in Table 3.

#### 5. Conclusion

With the PC1D numerical simulated program, the paper demonstrates the optimal magnitudes of emitter thickness, base thickness, emitter dopant density and base dopant density are 0.1  $\mu\text{m}$ , 100  $\mu\text{m}$ ,  $10^{20} \text{ cm}^{-3}$  and  $5 \times 10^{16} \text{ cm}^{-3}$ . The paper also exhibits PC1D’s potential to be widely used in solar cell design process because of its efficiency and reliability.

#### Acknowledgements

It was appreciated that Tian Pu and Huan Du from SUMEC Group Corporation offered guidance on production parameters of the typical crystalline solar cell. Their generous help is a solid guarantee for the project proceeding smoothly.

This research did not receive any specific grant from funding agencies in the public, commercial, or not-for-profit sectors

#### References

- [1] A. Descoedres, Z.C. Holman, L. Barraud, S. Morel, S. De Wolf, C. Ballif, Efficient silicon heterojunction solar cells on n- and p-type wafers compared, *IEEE J. Photovolt.* 3 (2013) 83–89.
- [2] A. Richter, M. Hermle, S.W. Glunz, Reassessment of the limiting efficiency for crystalline silicon solar cells, *IEEE J. Photovolt.* 3 (2013) 1184–1191.
- [3] K. Masuko, M. Shigematsu, T. Hashiguchi, D. Fujishima, M. Kai, T. Yamaguchi, Y. Ichihashi, T. Yamanishi, T. Takahama, E. Maruyama, S. Okamoto, N. Yoshimura, T. Yamaguchi, Y. Ichihashi, T. Mishima, N. Matsubara, T. Yamanishi, T. Takahama, M. Taguchi, E. Maruyama, S. Okamoto, Achievement of more than 25%: conversion efficiency with crystalline silicon heterojunction Solar cell, *Photovolt. IEEE J.* 4 (2014) 1433–1435.
- [4] C. Battaglia, A. Cuevas, S. De Wolf, High-efficiency crystalline silicon solar cells: status and perspectives, *Energy Environ. Sci.* 9 (2016) 1552–1576.
- [5] D.T. Rover, P.A. Basore, G.M. Thorson, Solar cell modeling on personal computers, *IEEE Photovoltaic Specialists Conference vol. 18 (1985) 703–709.*



- [6] P.A. Basore, D.T. Rover, A.W. Smith, PC-1D version 2: enhanced numerical solar cell modelling, in: Conference Record of the Twentieth IEEE Photovoltaic Specialists Conference, 1988, pp. 389–396.
- [7] P.A. Basore, PC-1D version 3: improved speed and convergence, in: The Conference Record of the Twenty-Second IEEE Photovoltaic Specialists Conference - 1991, 1991, pp. 299–302.
- [8] P.A. Basore, D.A. Clugston, PC1D version 4 for windows: from analysis to design, in: Proceedings of 25th IEEE Photovoltaic Specialists Conference—1996, 1996, pp. 377–381.
- [9] D.A. Clugston, P.A. Basore, PC1D version 5: 32-bit solar cell modeling on personal computers, in: Conf. Rec. Twenty Sixth IEEE Photovolt. Spec. Conf.—1997, 1997, pp. 207–210.
- [10] S.-ichiro Sato, H. Miyamoto, M. Imaizumi, K. Shimazaki, C. Morioka, K. Kawano, T. Ohshima, Degradation modeling of InGaP/GaAs/Ge triple-junction solar cells irradiated with various-energy protons, *Sol. Energy Mater. Sol. Cells* 93 (2009) 768–773.
- [11] P.P. Altermatt, Models for numerical device simulations of crystalline silicon solar cells - A review, *J. Comput. Electron* (2011).
- [12] S. Sepeai, S.H. Zaidi, M.K.M. Desa, M.Y. Sulaiman, N.A. Ludin, M.A. Ibrahim, K. Sopian, Design optimization of bifacial solar cell by PC1D simulation, *Parameters* 3 (5) (2013).
- [13] M. Belarbi, A. Benyoucef, B. Benyoucef, Simulation of the solar cells with PC1D, application to cells based on silicon, *Adv. Energy: Int. J. (AEIJ)* 1 (3) (2014) 1–10.
- [14] A.B. Nawale, R.A. Kalal, A.R. Chavan, T.D. Dongale, R.K. Kamat, Numerical investigation of spatial effects on the silicon solar cell, *J. Nano-Electron. Phys.* 8 (2016).
- [15] P. Panek, The influence of the base material parameters on quantum and photoconversion efficiency of the Si solar cells, *Arch. Metall. Mater.* 61 (4) (2016) 1889–1894.
- [16] H. Haug, J. Greulich, PC1Dmod 6.2—improved simulation of c-Si devices with updates on device physics and user interface, *Energy Procedia* (2016) 60–68.
- [17] H. Fan, O. Willardson, O. Beer, in: R.K. Williamson, A.C. Beer (Eds.), *Semiconductors and Semimetals*, Academic Press, 1967, p. 409.
- [18] Z.Z. Bandic, P.M. Bridger, E.C. Piquette, T.C. McGill, Electron diffusion length and lifetime in p-type GaN, *Appl. Phys. Lett.* 73 (1998) 3276.
- [19] Honsberg Christiana, Stuart Bowden, "Collection Probability", *Collection Probability | PVEducation*, [pveducation.org/pvcdrom/collection-probability](http://pveducation.org/pvcdrom/collection-probability) (Accessed 25 January 2018).
- [20] S.R. Wenham, M.A. Green, M.E. Watt, R. Corkish, A. Sproul, *Applied Photovoltaics*, Routledge, New York, USA, 2012.